Engineering Model of Surface Specularity: Spacecraft Design Implications

R. P. Bobco* and B. L. Drolen†
Hughes Aircraft Company, Los Angeles, California

Spacecraft thermal design relies on radiative transfer computer codes based on the concept of diffuse and specular components of surface hemispherical reflectance. This study describes an engineering model of bidirectional reflectance that leads to a simple two-parameter definition of specularity (ratio of specular component to hemispherical reflectance). The parameters are observable from bidirectional reflectance data for normal incidence and are the ratio of specular peak magnitude to uniform base magnitude (bimodal ratio) and the half-angle subtended by the specular peak. Normal directional reflectance is introduced as a scale factor. Directional variations of the peak bidirectional reflectance and the conical half-angle are postulated to allow separable, successive integrations over emergent and incident half-space to obtain approximate closed-form expressions for the diffuse and specular components of hemispherical reflectance and specularity. Numerical evaluation shows that specularity is a strong increasing function of both bimodal ratio and conical half-angle.

Nomenclature

A = area
D = detector signal, Ref. 10
F_{jk} = shape factor coupling A_j and A_k
i' = directional radiation intensity
i'' = bidirectional radiation intensity
J = integral in specular solid angle, Eq. (13)
N = bimodal ratio, peak bidirectional reflectance to base bidirectional reflectance, ρ''_m/ρ''_b
q'_{i2} = reflected irradiation at dA_2 based on bimodal model
$\hat{q}'_{i2}$ = reflected irradiation at dA_2 based on diffuse-plus-specular model
S = solar or beam collimated flux density, w/m^2
s = direction vector
V = instrument readout voltage, Ref. 11
$\beta(\theta_i)$ = cone semivertex angle associated with specular direction, Eq. (22)
Γ = irradiation ratio, $\hat{q}'_{i2}/q'_{i2}$
δ = bimodal residue parameter, Eq. (18)
$\delta(\pi/2,\theta_i)$ = Kronecker delta
θ = polar angle
$\bar{\theta}$ = bimodal model consistency limit for large angles of incidence
$\bar{\theta}_o$ = cone semivertex angle at normal incidence ($\theta_i = 0$)
v_o = cosine complement, Eq. (23)
ρ'' = dimensional bidirectional reflectance, sr^{-1}
ρ' = nondimensional directional reflectance
ρ = nondimensional hemispherical reflectance
$\hat{\sigma}$ = bimodal specularity; ratio of specular component to hemispherical reflectance, Eq. (31)
ϕ = azimuthal angle
ω,Ω = solid angles

Subscripts

b = uniform base value
d = diffuse
dh = directional-hemispherical
h = hemispherical
i = incident
m = specular
o = normal incidence ($\theta_i = 0$)
r = reflected
λ = monochromatic

Received April 22, 1988; presented as Paper 88-2723 at the AIAA Thermophysics Conference, San Antonio, TX, June 1988; revision received July 27, 1988.

*Senior Scientist. Associate Fellow AIAA.
†Senior Staff Engineer. Member AIAA.

Introduction

THERMAL design of space systems relies heavily on radiative transfer codes based on a surface reflectance model that decomposes hemispherical reflectance into diffuse and specular components, $\rho = \rho_d + \rho_m$. The two-component model of hemispherical reflectance was postulated by Seban[1] in 1962, but no guidelines were given for the relationship between the diffuse and specular components. Since that time, the diffuse-plus-specular model has been adapted to enclosure analysis implicit in the script-F radiation interchange factor, $\mathscr{F}_{ij}$.[2,3] Despite the wide acceptance of the two-component reflectance model, no progress has been made in specifying the magnitudes of ρ_d and ρ_m for common spacecraft thermal control surfaces. It is incumbent on the thermal analyst/designer to estimate ρ_d and ρ_m based on knowledge of hemispherical (or directional-hemispherical) reflectance, visual inspection of a surface, and experience. Subjective estimates of specularity appear to be acceptable for spacecraft interior analyses, but a more definitive characterization is required for many exterior applications. In particular, thermal control of external payloads may be compromised if solar or directed beam energy is focused on sensitive areas by specular reflection from remote surfaces.

A more rigorous analysis of radiation interchange, based on bidirectional reflectance, was reported by Bobco[4] in 1971. Bidirectional reflectance is a measurable surface property, but it has not been popularly accepted by spacecraft thermal analysts for a variety of reasons: unlike directional reflectances, bidirectional reflectance is both difficult to measure and requires multiple tables or graphs to present data for a single surface finish. For most engineering surfaces, bidirectional reflectance is a spectral property that is a strong function of incident and emergent angles. To date, no compendium has been published that presents integrated bidirectional reflectance data for either the solar waveband ($0 < \lambda \leqslant 3.0\ \mu$m) or the thermal waveband ($3.0 < \lambda \leqslant \sim 100\ \mu$m). The complexity and paucity of bidirectional reflectance data, coupled with the tedium of adapting it to script-F calculations, have obviated its use for thermal applications.

The work reported here provides an approximation that relates monochromatic bidirectional reflectance to hemispherical reflectance and leads to a rational approach for finding diffuse and specular components of reflectance. The bidirectional reflectance model and the diffuse-plus-specular model are compared by using each to calculate the irradiation at a differential target viewing a reflecting surface. The comparison illustrates the potential errors inherent in the diffuse-plus-specular model of surface reflectance.

Background

The literature of radiation heat transfer contains numerous entries on the subject of bidirectional or biangular reflectance but very little data on properties of engineering surfaces. Many of the measurements reported in the 1960's and 1970's were made on specially prepared surfaces to examine the influence of surface roughness and wavelength on bidirectional reflectance.[5-8] These studies were fundamental in character and had as a goal the development of a mathematical model for predicting bidirectional reflectance from other surface properties. A general model has yet to be developed, so engineering thermal analysts concerned with bidirectional reflectance effects must obtain data experimentally.

Typical of the data available for commercial applications are figures and tables in Refs. 9–11. Each of the references includes bidirectional data on the reflectance of a silicone-based white paint: S13 in Ref. 9, S13-G in Ref. 10, and S13-GLO in Ref. 11. It is believed that the three paints are similar, but the references do not include a description of the composition, method of application, thickness of layer, or other parameters that influence its reflective properties. Selected data for these paints are shown here in Figs. 1–3. Even a casual examination discloses considerable differences in the data formats.

The apparent differences among the three sets of data include normalizing factors, test specimen projected areas, wavelengths, and reference values. A tacit difference is the detector field of view, i.e., the solid angle of reflected energy that influences the angular resolution of data points. The definition of bidirectional reflectance presented by Siegel and Howell in Ref. 12 is used in the present study:

$$\rho''_\lambda(\theta_r,\phi_r,\theta_i,\phi_i) = \frac{i''_{\lambda r}(\theta_r,\phi_r,\theta_i,\phi_i)}{i'_{\lambda i}(\theta_i,\phi_i)\cos\theta_i\, d\omega_i},\ sr^{-1} \tag{1}$$

In Eq. (1), ρ'' is a dimensional quantity expressed in units of reciprocal steradians. In contrast, the bidirectional reflectance data in Fig. 1 is nondimensional and is given the symbol r''; the two reflectances are related as

$$r''_\lambda(\theta_r,\phi_r,\theta_i,\phi_i) = \pi\rho''_\lambda(\theta_r,\phi_r,\theta_i,\phi_i) \tag{2}$$

The data presented in Figs. 2 and 3 depict the angular distribution (plane of incidence) of reflected energy rather

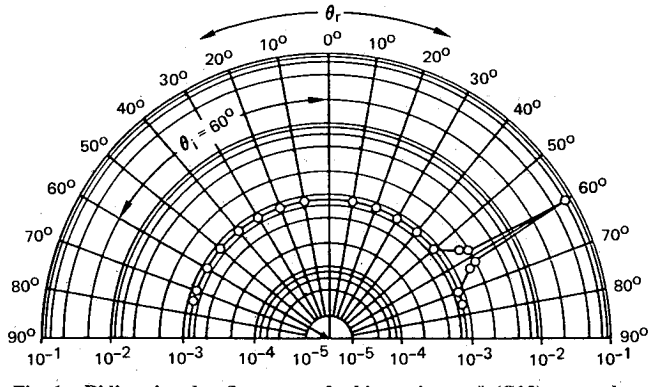

Fig. 1 Bidirectional reflectance of white paint $\pi\rho''$ (S13) monochromatic radiation ($\lambda = 0.5\ \mu m$) incident at $\theta_i = 60$ deg, $\phi_i = 0$ deg.[9]

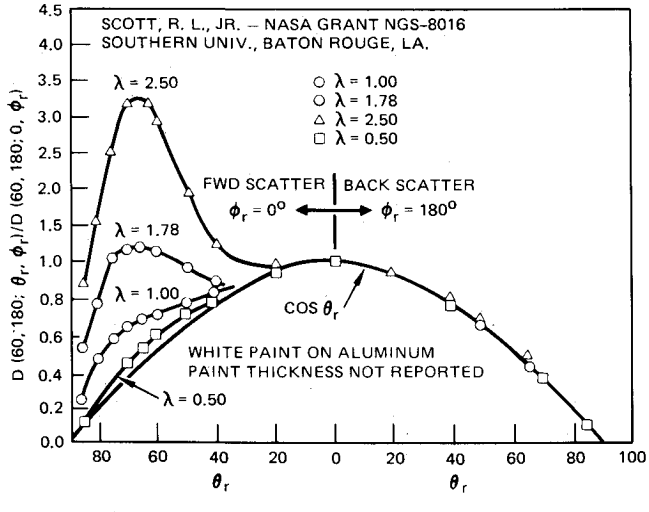

Fig. 2 Bidirectional reflection function of white paint (S13G) for 4 wavelengths; radiation incident at $\theta_i = 60$ deg, $\phi_i = 180$ deg.[10]

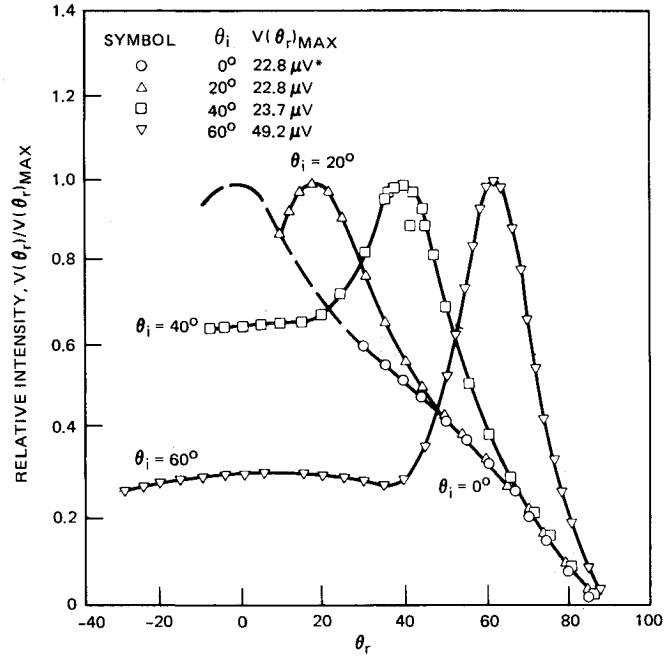

Fig. 3 Bidirectional reflection function of white paint (S13GLO); monochromatic radiation ($\lambda = 0.6\ \mu m$) incident at four different polar angles.[11]

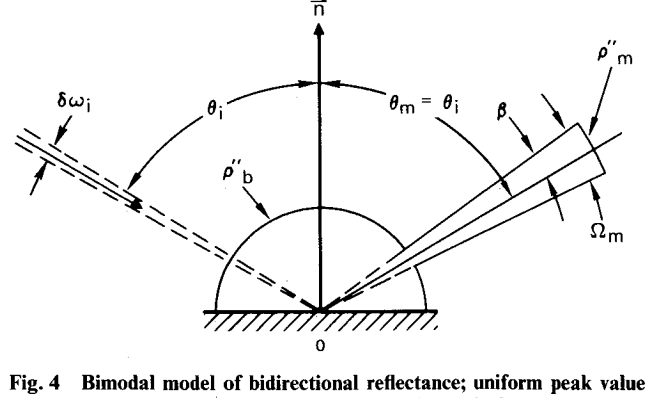

Fig. 4 Bimodal model of bidirectional reflectance; uniform peak value ρ''_m centered around specular direction within conical solid angle of semivertex angle β; uniform base reflectance ρ''_b in all other directions.

than bidirectional reflectances. Neither spectral reference parameters nor instrument factors are presented in Refs. 10 and 11; it is not apparent how the bidirectional distributions in Figs. 2 and 3 can be used directly for thermal design applications.

The data format of Figs. 2 and 3 is somewhat misleading insofar as a Lambertian, i.e., perfectly diffuse, surface is shown in Fig. 2 as a simple cosine of the reflection angle θ_r. This format tends to mask the existence of off-specular peak values of reflectance[13] at low wavelengths and high angles of incidence. For example, in Fig. 2, for radiation at 60 deg incidence with $\lambda = 1.78$ and 2.50 μm, it is apparent that a peak value of the reflection function occurs at 70–75 deg; however, for $\lambda = 0.50$ and 1.00 μm, the reflection function appears to decrease monotonically with increasing θ_r. Examination of the data shows that at $\lambda = 0.50$ μm, the bidirectional reflectance peak occurs at about $\theta_r = 75$ deg. In Fig. 3, however, there is only a slight suggestion of off-specular peaks.

Another feature that diminishes the usefulness of all the test data in Figs. 1–3 is the limited spectral scope of the reflection functions. For thermal design applications, it is necessary to use total values of absorptance and emittance appropriate to the waveband of interest. That is, in the solar waveband, the total bidirectional reflectance must be found from the expression

$$\rho''_{\text{solar}}(\theta_r,\phi_r,\theta_i,\phi_i) = \frac{1}{S}\int_0^\infty \rho''_\lambda(\theta_r,\phi_r,\theta_i,\phi_i) S_\lambda \, d\lambda \tag{3}$$

where S_λ is the spectral solar flux and S is the solar constant. Monochromatic bidirectional reflectance data is suitable only for laser irradiation heat balances.

Bidirectional reflectance data,[9-11] indicate that the bidirectional function for the three S13 paints is typical for most engineering surfaces. Most engineering surfaces exhibit a strong peak value of reflectance in the vicinity of the specular direction with a nearly uniform base value in all other directions; the bidirectional function decreases from the peak value to the base value within a comparatively small solid angle. This observation suggests that bidirectional reflectance rather than hemispherical reflectance may be modeled in terms of diffuse and specular components. The following presentation postulates a simple, bimodal, bidirectional reflectance model and examines its consequences with respect to the diffuse-plus-specular model of hemispherical reflectance.

Analysis

For notational convenience, the polar and azimuthal angles required to describe a direction will be embedded in a direction vector

$$\boldsymbol{s} = \boldsymbol{i}(\sin\theta\cos\phi) + \boldsymbol{j}(\sin\theta\sin\phi) + \boldsymbol{k}(\cos\phi) \tag{4}$$

With this notation, the argument required to express bidirectional reflectance is reduced to $(\boldsymbol{s}_r,\boldsymbol{s}_i)$; i.e.,

$$\rho''(\theta_r,\phi_r,\theta_i,\phi_i) = \rho''(\boldsymbol{s}_r,\boldsymbol{s}_i) \tag{5}$$

The spectral dependence is dropped for convenience but implied in all that follows.

The relationships among bidirectional, directional, and hemispherical reflectances are given in Ref. 12:

Directional-hemispherical reflectance:

$$\rho'_{dh}(\boldsymbol{s}_i) = \int_{(2\pi)_r} \rho''(\boldsymbol{s}_r,\boldsymbol{s}_i)\cos\theta_r \, d\omega_r \tag{6}$$

Hemispherical-directional reflectance:

$$\rho'_{hd}(\boldsymbol{s}_r) = \int_{(2\pi)_i} \rho''(\boldsymbol{s}_r,\boldsymbol{s}_i)\cos\theta_i \, d\omega_i \tag{7}$$

Hemispherical reflectance:

$$\rho_h = \frac{1}{\pi}\int_{(2\pi)_i} \rho'_{dh}(\boldsymbol{s}_i)\cos\theta_i \, d\omega_i \tag{8a}$$

$$= \frac{1}{\pi}\int_{(2\pi)_r} \rho'_{hd}(\boldsymbol{s}_r)\cos\theta_r \, d\omega_r \tag{8b}$$

The reflectances ρ'_{dh}, ρ'_{hd}, and ρ_h are nondimensional. It will be shown how Eqs. 6–8 may be used to evaluate diffuse and specular components of hemispherical reflectance when $\rho''(\boldsymbol{s}_r,\boldsymbol{s}_i)$ has an analytically tractable form.

The bidirectional reflectance data for white paint exhibit a bimodal character: the magnitude of $\rho''(\boldsymbol{s}_r,\boldsymbol{s}_i)$ is greater in a solid angle in the vicinity of the specular direction than in the remaining half-space. This observation suggests that the half-space for reflected energy may be decomposed into two solid angles,

$$\Omega_m + \Omega_b = (2\pi)_r \tag{9}$$

where Ω_m is the solid angle including the specular direction and Ω_b is the remaining half-space. The bidirectional reflectance may be represented by different functions in each solid angle,

$$\rho''(\boldsymbol{s}_r,\boldsymbol{s}_i) = \rho''_m(\Omega_m,\boldsymbol{s}_i), \qquad \rho''(\boldsymbol{s}_r,\boldsymbol{s}_i) = \rho''_b(\Omega_b,\boldsymbol{s}_i) \tag{10}$$

where $\rho''_m(\Omega_m,\boldsymbol{s}_i) \geq \rho''_b(\Omega_b,\boldsymbol{s}_i)$ in all directions $\boldsymbol{s}_r$. Additionally, the data suggest that Ω_m depends on the incident direction so that $\Omega_m = \Omega_m(\boldsymbol{s}_i)$ insofar as the specular direction $\boldsymbol{s}_m$ is completely defined when $\boldsymbol{s}_i$ is specified. From this, it follows that

$$\rho''(\boldsymbol{s}_r,\boldsymbol{s}_i) = \rho''_m[\Omega_m(\boldsymbol{s}_i),\boldsymbol{s}_i] = \rho''_m(\boldsymbol{s}_i) \quad \text{in} \quad \Omega_m(\boldsymbol{s}_i) \tag{11a}$$

$$\rho''(\boldsymbol{s}_r,\boldsymbol{s}_i) = \rho''_b[\Omega_b(\boldsymbol{s}_i),\boldsymbol{s}_i] = \rho''_b(\boldsymbol{s}_i) \quad \text{in} \quad \Omega_b(\boldsymbol{s}_i) \tag{11b}$$

Equation (11) may be introduced in Eq. (6) to find

$$\rho'_{dh}(\boldsymbol{s}_i) = \int_{\Omega_m} \rho''_m(\boldsymbol{s}_i)\cos\theta_r \, d\omega_r + \int_{\Omega_b} \rho''_b(\boldsymbol{s}_i)\cos\theta_r \, d\omega_r$$

or, alternatively, assuming the existence of $\rho''_b(\boldsymbol{s}_i)$ in $\Omega_m(\boldsymbol{s}_i)$,

$$\rho'_{dh}(\boldsymbol{s}_i) = \int_{(2\pi)_r} \rho''_b(\boldsymbol{s}_i)\cos\theta_r \, d\omega_r + \int_{\Omega_m(\boldsymbol{s}_i)} [\rho''_m(\boldsymbol{s}_i) - \rho''_b(\boldsymbol{s}_i)]\cos\theta_r \, d\omega_r$$

Observe that $\rho''_m(\boldsymbol{s}_i)$ and $\rho''_b(\boldsymbol{s}_i)$ are functions of incident direction only, while the integration is over emergent directions. In this instance, the integrals reduce to the simpler form

$$\rho'_{dh}(\boldsymbol{s}_i) = \pi\rho''_b(\boldsymbol{s}_i) + [\rho''_m(\boldsymbol{s}_i) - \rho''_b(\boldsymbol{s}_i)]\int_{\Omega_m(\boldsymbol{s}_i)} \cos\theta_r \, d\omega_r \tag{12}$$

The integral in Eq. (12) is a function of the incident directions implicit in $\Omega_m(\boldsymbol{s}_i)$ so that it may be expressed as

$$J_m(\boldsymbol{s}_i) = \int_{\Omega_m(\boldsymbol{s}_i)} \cos\theta_r \, d\omega_r \tag{13}$$

whereby

$$\rho'_{dh}(\boldsymbol{s}_i) = \rho''_b(\boldsymbol{s}_i)[\pi - J_m(\boldsymbol{s}_i)] + \rho''_m(\boldsymbol{s}_i)J_m(\boldsymbol{s}_i) \tag{14}$$

The directional-hemispherical reflectance in Eq. (14) is seen to be decomposed into two components that depend on the incident direction only.

Hemispherical reflectance follows from Eqs. (8a) and (14)

by integrating over all incident directions:

$$\rho_h = \frac{1}{\pi}\int_{(2\pi)_i} \rho'_{dh}(s_i)\cos\theta_i\, d\omega_i$$
$$= \frac{1}{\pi}\int_{(2\pi)_i} \rho''_b(s_i)[\pi - J_m(s_i)]\cos\theta_i\, d\omega_i$$
$$+ \frac{1}{\pi}\int_{(2\pi)_i} \rho''_m(s_i)J_m(s_i)\cos\theta_i\, d\omega_i \qquad (15)$$

The first integral in Eq. (15) depends on the back- and side-scattering contribution to hemispherical reflectance, i.e., the nonspecular component. The second integral contains the specular contribution to hemispherical reflectance. On the basis of these observations, it is reasonable to define diffuse and specular components of hemispherical reflectance

$$\rho_h = \rho_d + \rho_m \qquad (16a)$$

where

$$\rho_d = \frac{1}{\pi}\int_{(2\pi)_i} \rho''_b(s_i)[\pi - J_m(s_i)]\cos\theta_i\, d\omega_i \qquad (16b)$$

$$\rho_m = \frac{1}{\pi}\int_{(2\pi)_i} \rho''_m(s_i)J_m(s_i)\cos\theta_i\, d\omega_i \qquad (16c)$$

The component definitions given by Eq. (16) are conceptually simple and reasonably general, but they are not entirely objective. The selection of a specular solid angle $\Omega_m(s_i)$ requires engineering judgment for some diffusing surfaces.

Engineering Model for Specularity

A hypothetical surface is postulated with an idealized bidirectional reflectance. Figure 4 shows the essential features of the bidirectional reflectance; the characteristics are more realistic than the idealized cases of diffuse, specular, or diffuse-plus-specular reflectance and lend themselves to substitution in Eq. (16). The specular peak $\rho''_m(\theta_i)$ is assumed to be uniform everywhere in a conical solid angle $\Omega_m(\theta_i)$ of semivertex angle $\beta(\theta_i)$. The bidirectional reflectance is assumed to have a second uniform value of lesser magnitude, $\rho''_b(\theta_i)$, in all other directions not included in $\Omega_m(\theta_i)$. The specular peak is assumed to be an increasing function of angle of incidence and to vary as

$$\rho''_m(\theta_i) = \rho''_{m,o}/(\cos^2\theta_i + \delta), \qquad \delta \ll 1 \qquad (17)$$

where δ is a residual parameter; δ is introduced to avoid singularities associated with θ_i approaching $\pi/2$. In the following numerical studies it is assumed that $\delta = 10^{-4}$. The conical solid angle is assumed to be a decreasing function of incidence angle and vary as

$$\Omega_m(\theta_i) = \Omega_{m,o}\cos\theta_i \qquad (18)$$

The postulated behavior of $\rho''_m(\theta_i)$ and $\Omega_m(\theta_i)$ is supported, qualitatively, by observed trends.

Presumably, $\rho''_{m,o}$, ρ_b, and $\Omega_{m,o}$ may be found empirically from bidirectional reflectance data measured at normal incidence, $\theta_i = 0$. It is convenient to introduce a bidirectional ratio

$$N = \rho''_{m,o}/\rho''_b \qquad (19)$$

In the following development, it will be shown how the parameters N, $\beta(0) = \bar{\theta}_o$, and the normal hemispherical reflectance $\rho'_{dh}(0) = \rho'_{dh,o}$ may be used to estimate diffuse and specular components of hemispherical reflectance and the specularity of a surface.

The magnitude of a conical solid angle is readily found in terms of its semivertex angle β, i.e.,

$$\Omega = \int_o^{2\pi}\int_o^{\beta} \sin\theta\, d\theta\, d\phi = 2\pi(1 - \cos\beta) \qquad (20)$$

where θ and ϕ are polar and azimuthal angles in an arbitrary coordinate system. In the present application, it is assumed that the semivertex angle corresponding to normal incidence $\bar{\theta}_o$ is known from empirical data so that

$$\Omega_{m,o} = 2\pi(1 - \cos\bar{\theta}_o) \qquad (21a)$$

The solid angle for arbitrary angle of incidence is

$$\Omega_m(\theta_i) = 2\pi[1 - \cos\beta(\theta_i)] \qquad (21b)$$

Combining Eqs. (18) and (21) leads to the expression

$$\cos\beta(\theta_i) = 1 - v_o\cos\theta_i \qquad (22)$$

where

$$v_o = 1 - \cos\bar{\theta}_o \qquad (23)$$

This definition of $\beta(\theta_i)$ shows that β decreases as θ_i increases toward 90 deg; however, anomalous behavior occurs in a small range $\bar{\theta}_i < \theta_i \le 90$ deg, where $\cos\bar{\theta}_i = 2v_o/(1 + v_o^2)$. In that range, the sum $[\theta_i + \beta(\theta_i)]$ exceeds 90 deg by a small amount. For example, when $\bar{\theta}_o = 30$ deg and $\theta_i = 86$ deg, Eq. (22) yields $\beta(\theta_i) = 7.84$ deg, whereby $[\theta_i + \beta(\theta_i)] = 93.84$ deg. This anomaly serves to accent the approximate nature of the engineering model.

Next, consider the integral $J_m(s_i)$ in Eq. (13). A rigorous integration over $\phi(\theta_i)$ and θ_i does not appear to be possible, but the mean value theorem may be invoked to obtain

$$J_m(s_i) = \int_{\Omega_m(s_i)} \cos\theta_r\, d\omega_r = \Omega_m(s_i)\,\overline{\cos\theta_r} \qquad (24)$$

where $\overline{\cos\theta_r}$ is the mean value in the solid angle. In Fig. 4, it may be seen that $[\theta_i - \beta(\theta_i)] < \theta_m \le [\theta_i + \beta(\theta_i)]$, so that the mean value may be approximated as

$$\overline{\cos\theta_r} = \tfrac{1}{2}\{\cos[\theta_i + \beta(\theta_i)] + \cos[\theta_i - \beta(\theta_i)]\}$$
$$= \cos\beta(\theta_i)\cos\theta_i = (1 - v_o\cos\theta_i)\cos\theta_i \qquad (25)$$

where use is made of Eq. (23). From Eqs. (18) and (21) et seq., it follows that $J_m(s_i)$ may be approximated as

$$J_m(s_i) = 2\pi v_o(1 - v_o\cos\theta_i)\cos^2\theta_i \qquad (26)$$

Introduce Eqs. (19) and (26) in Eq. (14) to obtain

$$\rho'_{dh}(s_i) = \rho'_{dh}(\theta_i)$$
$$= \pi\rho''_b\left\{1 + \left[\frac{2v_o\cos^2\theta_i(1 - v_0\cos\theta_i)(N - \cos^2\theta_i - \delta)}{\delta + \cos^2\theta_i}\right]\right\} \qquad (27)$$

If ρ''_b is known, Eq. (27) may be used to estimate the directional-hemispherical reflectance. In the present development, it is assumed that a measurement in an integrating sphere yields the normal reflectance $\rho'_{dh,o}$, so that ρ''_b may be estimated instead:

$$\pi\rho''_b = \rho'_{dh,o}\Big/\left[1 + \frac{2v_o(1 - v_o)(N - 1 - \delta)}{\delta + 1}\right] \qquad (28)$$

From Eqs. (27) and (28), it follows that directional-hemi-

spherical reflectance takes the form

$$\rho'_{dh}(\theta_i) = \rho'_{dh,o}\left\{\left[\frac{\delta+1}{\delta+\cos^2\theta_i}\right] \times \left[\frac{\delta+\cos^2\theta_i[1+2v_o(1-v_o\cos\theta_i)(N-\cos^2\theta_i-\delta)]}{\delta+[1+2v(1-v)(N-1-\delta)]}\right]\right\} \quad (29)$$

The integration over all incident directions to obtain diffuse and specular components of hemispherical reflectance is straightforward using Eq. (26) in Eq. (16):

$$\rho_d = \rho'_{dh,o}\left\{\frac{(\delta+1)[1-v_o(1-4v_o/5)]}{\delta+1+2v_o(1-v_o)(N-1-\delta)}\right\} \quad (30a)$$

$$\rho_m = \rho'_{dh,o}\left\{\frac{2v_oN(\delta+1)(1-2v_o/3+\delta\{\ell n[\delta/(1+\delta)]+2v_o[1-\delta^{1/2}\tan^{-1}(1/\sqrt{\delta})]\})}{\delta+1+2v_o(1-v_o)(N-1-\delta)}\right\} \quad (30b)$$

$$\rho_h = \rho'_{dh,o}\left\{\frac{(\delta+1)\{[1-v_o(1-4v_o/5)]+2v_oN(1-2v_o/3+\delta\{\ell n[\delta/(1+\delta)]+2v_o[1-\delta^{1/2}\tan^{-1}(1/\sqrt{\delta})]\})\}}{\delta+1+2v_o(1-v_o)(N-1-\delta)}\right\} \quad (30c)$$

The final parameter of interest is the ratio of specular reflectance to hemispherical reflectance, designated here as specularity $\hat{\sigma}$:

$$\hat{\sigma} = \rho_m/\rho_h \quad (31)$$

It may be observed that specularity does not depend on absolute values of bidirectional or directional-hemispherical reflectance. Specularity is a function of the bimodal parameters N and $\bar{\theta}_o$, both of which may be estimated from relative values of bidirectional reflectance measured at normal incidence.

Numerical Trends

The influence of N and $\bar{\theta}_o$ on base reflectance, directional-hemispherical reflectance, and specularity is illustrated in Figs. 5–7. The base reflectance and directional reflectance are normalized with respect to $\rho'_{dh,o}$. Results are shown for the following values of bimodal parameters: $N = 10, 10^2, 10^3, 10^4$, $0 < \bar{\theta}_o \leq 30$ deg. It is assumed that the residue parameter is $\delta = 10^{-4}$. Base reflectance (Fig. 5) decreases as both N and $\bar{\theta}_o$ increase. These curves suggest that diffuse transport becomes vanishingly small as reflected energy is concentrated in the conical solid angle. Figure 6 shows that the assumed variation of $\rho''_m(\theta_i)$ and $\Omega_m(\theta_i)$ leads to a small increase in directional reflectance as the angle of incidence approaches 90 deg. This trend appears to be a stronger function of the conical normal semivertex angle, $\bar{\theta}_o$, than the bimodal ratio, N. Experience indicates that real surfaces become more "reflective" at grazing incidence.

Surface specularity (Fig. 7) exhibits intuitive trends for large values of $N(=10^3$ and $10^4)$; however, the influence of conical normal semivertex angle $\bar{\theta}_o$ is unexpected. It appears that even a modest specular peak ($N = 10$) leads to large values of specularity ($\hat{\sigma} \geq 0.50$) for $\bar{\theta}_o \geq 16$ deg. This behavior suggests that surface treatments that attempt to diminish specularity by lowering N and broadening $\bar{\theta}_o$ may have only a marginal influence on specular focusing of incident radiation. The curves in Fig. 7 indicate that the specularity of a surface with $(N,\bar{\theta}_o) = (10^3, \sim 2.5$ deg) is equivalent to a surface for which $(N,\bar{\theta}_o) = (10, \sim 27.5$ deg); both surfaces have specularities of about 0.70.

In the following section, some of these results are used to formulate expressions for the reflected irradiation incident on a differential area viewing a semi-infinite plane irradiated by a collimated source. This simple geometry provides a convenient basis for estimating the propriety of the conventional diffuse-plus-specular model of surface reflectance.

Application to Reflected Irradiation

In Fig. 8, a semi-infinite plane A_1 is irradiated by a uniform, collimated flux S. A differential area dA_2 situated above the edge of and in a plane perpendicular to A_1 has an unobstructed view of A_1. The collimated flux is incident at A_1, with an angle θ_{s1} measured from the surface normal, $\boldsymbol{n}_1$. The specular angle, $\theta_m = \theta_{s1}$, is defined by a ray reflected from A_1 and incident on dA_2 at an angle $\theta_2 = \pi/2 - \theta_{s1}$. The surface A_1 is assumed to have a bidirectional reflectance $\rho''_1(s_i,s_r)$ that may be represented by the bimodal parameters N, $\bar{\theta}_o$; the normal hemispherical reflectance, $\rho'_{1dh,o}$, is assumed known.

The surface properties of dA_2 are arbitrary for the present consideration if it is assumed that radiative interaction between dA_2 and A_1 has a negligible influence on the radiant flux emerging from A_1.

The complete radiant flux incident at dA_2 consists of a direct flux $S\cos\theta_{s2}$ and a flux reflected from A_1. The reflected flux, designated q'_{i2} and called the reflected irradiation at dA_2, is the parameter of interest here. If A_1 is assumed to have diffuse and specular components of hemispherical reflectance ρ_{d1} and ρ_{m1}, respectively, the reflected irradiation is formulated as

$$q'_{i2} = \rho_{d1}F_{21}S\cos\theta_{s1} + [1-\bar{\delta}(\pi/2, \theta_{s1})]\rho_{m1}S\cos\theta_2 \quad (32)$$

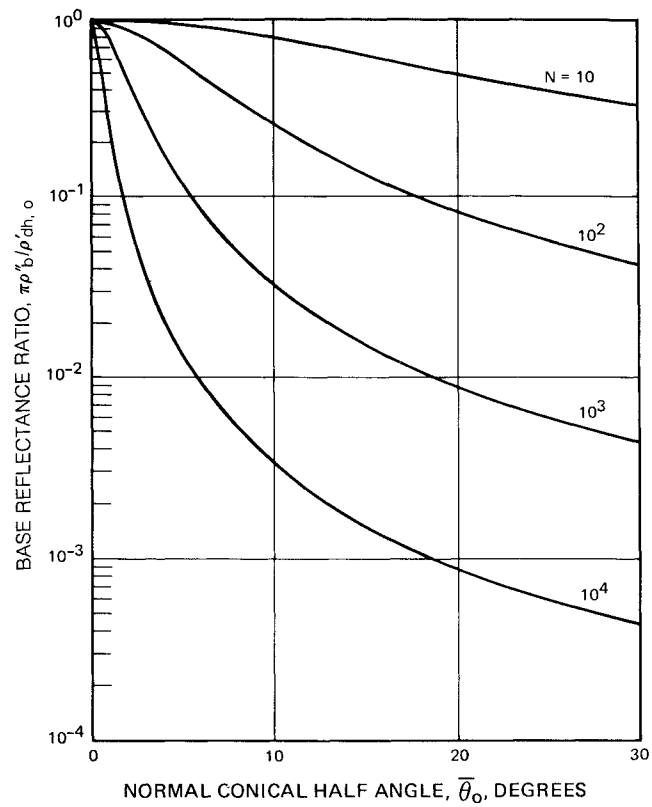

Fig. 5 Base reflectance ρ''_b as function of specular peak normal conical half-angle $\bar{\theta}_o$ and normal peak-to-base ratio N.

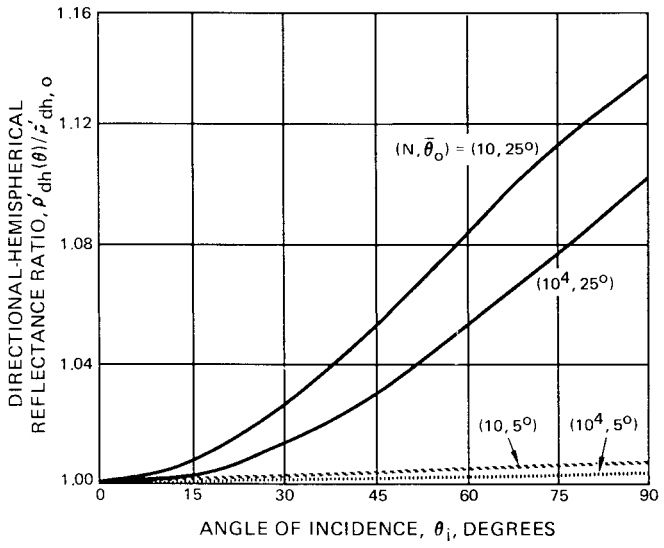

Fig. 6 Directional hemispherical reflectance $\rho'_{dh}(\theta_i)$ as function of incident polar angle for selected values of normal cone half-angle $\bar{\theta}_o$ and normal peak-to-base ratio N.

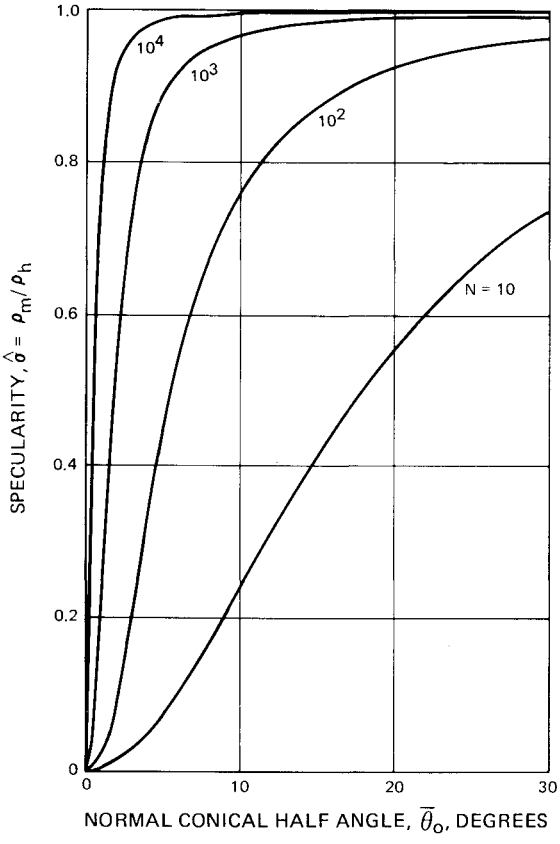

Fig. 7 Specularity $\hat{\sigma}$ as function of normal conical half-angle $\bar{\theta}_o$ and normal peak-to-base ratio N.

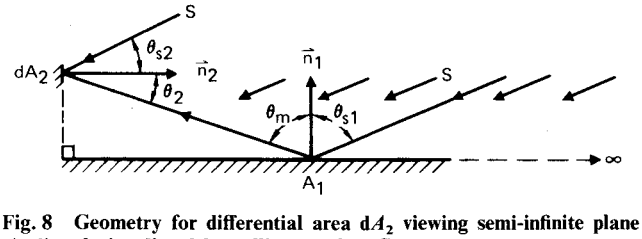

Fig. 8 Geometry for differential area dA_2 viewing semi-infinite plane A_1 directly irradiated by collimated flux S.

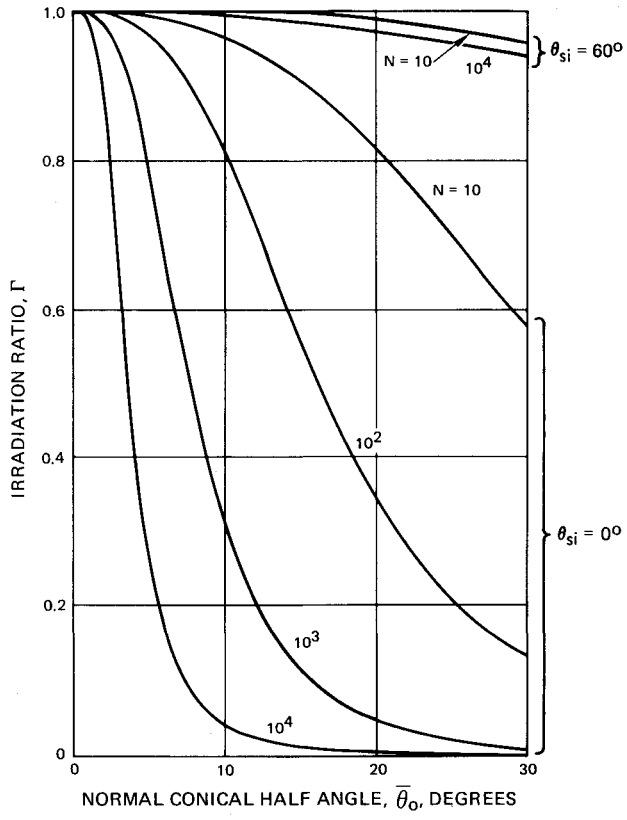

Fig. 9 Comparison of diffuse-plus-specular model of hemispherical reflectance and bimodal bidirectional reflectance model; irradiation ratio as function of normal cone half-angle $\bar{\theta}_o$ and bimodal ratio N for selected values of incident radiation.

The parameter $\hat{\delta}(\pi/2, \theta_{s1})$ is the Kronecker delta for which

$$\hat{\delta}(\pi/2, \theta_{s1}) = 0, \qquad \theta_{s1} \neq \pi/2$$

$$= 1, \qquad \theta_{s1} = \pi/2$$

Introduce Eqs. (29a) and (29b) into Eq. (32) and observe $F_{21} = \frac{1}{2}$ and $\cos\theta_2 = \sin\theta_{s1}$ to obtain

$$q'_{i2} = \frac{(\delta+1)\rho'_{dh,o} S \cos\theta_{s1}}{\delta + 1 + 2\nu_o(1-\nu_o)(N-1-\delta)} \{\tfrac{1}{2}[1 - \nu_o(1 - 4\nu_o/5)] + [1 - \hat{\delta}(\pi/2, \theta_{s1})] \tan\theta_{s1}[2\nu_o N(1 - 2\nu_o/3 + \delta \times \{\ell n[\delta/(1+\delta)] + 2\nu_o[1 - \delta^{1/2}\tan^{-1}(1/\sqrt{\delta})]\})]\} \tag{33}$$

Equation (33) defines the irradiation at dA_2 when A_1 is assumed to have diffuse and specular components of reflectance that are defined by Eqs. (30a) and (30b).

A more rigorous expression for the irradiation at dA_2 may be obtained in terms of the assumed bidirectional reflectance $\rho''_1(\theta_{si})$. In Ref. 14, it is shown that the reflective irradiation may be expressed as

$$q'_{i2} = S \cos\theta_{s1} \int_{\Omega_{21}} \rho''_1 \cos\theta \, d\omega \tag{34}$$

where Ω_{21} represents the solid angle subtended by A_1 at dA_2 and θ is the angle of incidence at dA_2. Recognizing that $dF_{12} = \cos\theta \, d\omega/\pi$, rearrange Eq. (34) to obtain

$$q'_{i2} = \pi S \cos\theta_{s1} \int_{A_1} \rho''_1 \, dF_{21}$$

$$= \pi S \cos\theta_{s1} \left[\int_{A_{1b}} \rho''_{1b} \, dF_{2,1b} + \int_{A_{1m}} \rho''_{1m} \, dF_{2,1m} \right] \tag{35}$$

where $A_{1b} + A_{1m} = A_1$. For a bimodal model with $N = \rho''_{m,o}/\rho''_b > 1$, an observer at dA_2 perceives the radiation emerging from A_1 as a bright elliptical area A_{1m} and a uniform, less bright area everywhere else. From this observation, it follows that

$$q'_{i2} = \pi S \cos\theta_{s1}[\rho''_{1b}F_{2,1b} + \rho''_{1m}F_{2,1m}] \tag{36}$$

For a semi-infinite A_1, $F_{2,1b} + F_{2,1m} = \frac{1}{2}$, so that Eq. (36) may be rearranged as

$$q'_{i2} = \pi\rho''_{1b}S \cos\theta_{s1}\left[\frac{(\frac{1}{2})(\delta + \cos^2\theta_{s1}) + F_{2,1m}(N - \cos^2\theta_{s1} - \delta)}{\delta + \cos^2\theta_{s1}}\right] \tag{37}$$

Using Eq. (27), Eq. (37) becomes

$$q'_{i2} = \frac{(1+\delta)\rho'_{dh,o}S\cos\theta_{s1}}{[\delta + 1 + 2v_o(1 - v_o)(N - 1 - \delta)]} \times \left[\frac{(\frac{1}{2})(\delta + \cos^2\theta_{s1}) + F_{2,1m}(N - \cos^2\theta_{s1} - \delta)}{\delta + \cos^2\theta_{s1}}\right] \tag{38}$$

The remaining discussion will examine the irradiation ratio

$$\Gamma = \hat{q}'_{i2}/q'_{i2} \tag{39}$$

to assess the propriety of the diffuse-plus-specular model of surface reflectance.

The shape factor $F_{2,1m}$ depends on the incidence angle θ_{s1}. An observer at dA_2 viewing A_{1m} see a complete ellipse for $\bar{\theta}_o \le \theta_{s1} < \pi/2$ and a partial ellipse for $\theta_{s1} < \bar{\theta}_o$ that reduces to a semicircle at $\theta_{s1} = 0$. The shape factor to the full ellipse is easily found (e.g., unit sphere method) as

$$F_{2,1m} = \sin^2\beta(\theta_{s1})\sin\theta_{s1}, \qquad \bar{\theta}_o \le \theta_{s1} \le \pi/2$$
$$= v_o \sin\theta_{s1}\cos\theta_{s1}(2 - v_o\cos\theta_{s1}) \tag{40a}$$

For $\theta_{s1} < \bar{\theta}_o$, presumably contour integration may be used to obtain a suitable expression; when $\theta_{s1} = 0$, the shape factor is

$$F_{2,1m} = (1/\pi)(\bar{\theta}_o - \sin\bar{\theta}_o\cos\bar{\theta}_o), \qquad \theta_{s1} = 0 \tag{40b}$$

Equation (40) was used in Eq. (39) to obtain the results shown in Fig. 9 and Table 1.

Discussion

The irradiation ratio trends (Fig. 9 and Table 1) show that the agreement between the diffuse-plus-specular model and the bimodal bidirectional model is quite good for most applications. It may be established that the two models are in good agreement, e.g., $\Gamma = 1 \pm 0.06$, for $\bar{\theta}_o < \theta_{si} \le \bar{\theta}_{si}$. The diffuse-plus-specular model underpredicts ($\Gamma < 1$) considerably for the case of the normal solar incidence ($\theta_{s1} = 0$) because no account is taken of energy divergence in the solid angle Ω_m. For example, at normal incidence, the specular component of reflected energy is parallel to dA_2; hence, no specularly reflected energy is incident at the target dA_2. On the other hand, the bimodal model allows specular reflected energy to emerge from A_1 within a divergent solid angle of semi-vertex angle $\bar{\theta}_o$ and to be incident at dA_2. The phenomenon is comparable to beam divergence in solar simulators,[15] where imperfect collimation causes direct irradiation at surfaces intended to be parallel to the solar direction. The divergence problem is strongly dependent on geometry and surface properties (α/ε ratio). The present study merely identifies a narrow range of incidence angles where conventional diffuse-plus-specular analysis underpredicts irradiation. Additional study is required to identify circumstances in which the diffuse-plus-specular model is inadequate.

Table 1 Irradiation ratio Γ: residual, $\delta = 10^{-4}$

		Γ			
θ_{s1}	$\bar{\theta}_o$	$N = 10^4$	$N = 10^3$	$N = 10^2$	$N = 10$
0	0	1.0000	1.0000	1.0000	1.0000
	10	0.0421	0.3040	0.8061	0.9655
	20	0.0053	0.0507	0.3435	0.8136
	30	0.0015	0.0150	0.1312	0.5796
30	0	1.0000	1.0000	1.0000	1.0000
	10	0.9957	0.9961	0.9991	1.0073
	20	0.9848	0.9852	0.9887	1.0105
	30	0.9660	0.9664	0.9701	0.9999
60	0	1.0000	1.0000	1.0000	1.0000
	10	0.9931	0.9933	0.9947	1.0020
	20	0.9740	0.9741	0.9756	0.9877
	30	0.9417	0.9419	0.9436	0.9571

The current bimodal bidirectional model appears to be consistent and useful for examining reflected irradiation effects for solar or beam incidence angles in the range $0 \le \theta_{si} \le \bar{\theta}_{si}$. In the complementary range, $\bar{\theta}_{si} < \theta_{si} \le \pi/2$, the bimodal model should be used with caution. Experimental difficulties usually prevent measurements of bidirectional reflectance at grazing incidence and analytical models based on more fundamental considerations are not useful for engineering applications. As a result, it is not possible to evaluate the propriety of the bimodal model at large angles of incidence. Equation (39) is well behaved in the complementary range, $\bar{\theta}_{si} < \theta_{si} \le \pi/2$, but it cannot be verified at this time.

The present study is exploratory insofar as it verifies the usefulness of the conventional diffuse-plus-specular model of surface reflectance for a large range of solar or beam incidence angles, and it provides a succinct definition of specularity. A data base of total values of N and $\bar{\theta}_o$ for common surfaces is required to make the present observations useful for thermal design applications. In the absence of such a compendium, the thermal designer must seek bidirectional data available in the literature and use engineering judgment to estimate N and $\bar{\theta}_o$ for use in specifying surface specularity and the diffuse and specular components of hemispherical reflectance.

Summary and Conclusions

The work reported here provides an approximate, quantitative relationship between surface bidirectional reflectance and the previously intuitive concept of surface specularity. An engineering model of bidirectional reflectance was postulated in terms of variable peak (specular) and uniform base (diffuse) components and a variable conical solid angle, defined by a variable semi-vertex angle; normal hemispherical reflectance was selected as a convenient scale factor. The model, designated bimodal bidirectional reflectance, is fully described by two observable parameters. An approximate integration leads to a simple expression for directional-hemispherical reflectance; a second exact integration provides another simple expression for hemispherical reflectance. Specularity, defined as the ratio of specular component reflectance to hemispherical reflectance, is shown to depend on the ratio of peak-to-base bidirectional reflectances and the cone half-angle observed at normal incidence. Numerical investigation shows that specularity is a strong function of both the peak-to-base ratio and the cone half-angle. An unexpected finding is that specularity increases with increasing conical half-angle.

A simple geometry was used to formulate incident-reflected flux at a differential area and compare the irradiation from a diffuse-plus-specular surface and a bimodal bidirectional surface. Analysis shows agreement between the two models of surface reflectance and supports the continued use of computer codes based on the diffuse-plus-specular model of surface

reflectance. A potential problem with the diffuse-plus-specular model may arise at near normal angles of solar or beam incidence; it is shown that reflected irradiation is underpredicted at surfaces parallel to the beam for this condition.

The principal conclusion of this study is that the diffuse-plus-specular model of surface reflectance is adequate for thermal analysis and design of many exterior spacecraft subsystems. Unfortunately, this observation cannot be used to advantage without a data base of surface properties that includes specularity. Additional research is required to measure, analyze, and compile monochromatic and total solar bidirectional characteristics of spacecraft surfaces, infer bimodal parameters, and determine their specularity.

References

[1]Seban, R., "Discussion of 'An Enclosure Theory for Radiative Exchange Between Specularly and Diffusely Reflecting Surfaces' by Sparrow, E. M., Eckert, E. R. G., and Jonsson, V. K.," *Journal of Heat Transfer*, Vol. 84C, No. 4, Nov. 1962, pp. 299–300.

[2]Sparrow, E. M. and Lin, S. L., "Radiation Heat Transfer at a Surface Having Both Specular and Diffuse Reflectance Components," *International Journal of Heat and Mass Transfer*, Vol. 8, 1965, pp. 769–778.

[3]Sarofim, A. F. and Hottel, H. C., "Radiative Exchange Among Non-Lambert Surfaces," *Journal of Heat Transfer*, Vol. 88, Feb. 1966, pp. 37–44.

[4]Bobco, R. P., "A Script-F Matrix Formulation for Enclosures with Arbitrary Surface Emission and Reflection Characteristics," *Journal of Heat Transfer*, Vol. 93C, No. 1, Feb. 1971, pp. 33–40.

[5]Bennett, H. E. and Porteus, J. O., "Relation Between Surface Roughness and Specular Reflectance at Normal Incidence," *Journal of the Optical Society of America*, Vol. 51, Feb. 1961, pp. 123–129.

[6]Birkebak, R. C. and Eckert, E. R. G., "Effects of Roughness of Metal Surfaces on Angular Distribution of Monochromatic Reflected Radiation," *Journal of Heat Transfer*, Vol. 87, Feb. 1965, pp. 85–94.

[7]Torrance, K. E. and Sparrow, E. M., "Biangular Reflectance of an Electric Non-Conductor as a Function of Wavelength and Surface Roughness," *Journal of Heat Transfer*, Vol. 87, May 1965, pp. 283–292.

[8]Smith, T. F. and Hering, R. G., *Surface Roughness Effects on Bidirectional Reflectance*, Univ. of Illinois Heat Transfer Lab., Urbana-Champaign, ME-TR-661-2, UILU-ENG-72-4001, 1972.

[9]Miller, W. D., "A Report on the Visual Bidirectional Reflectance Properties of Selected Apollo Materials," TRW, Redondo Beach, CA, Rept. 68-3346.11u-30, NASA NAS9-5073, April 1968.

[10]Scott, R. L., Jr., "Bidirectional Reflectance Study," Dept. of Mechanical Engineering, Southern Univ., Baton Rouge, LA, Final Rept. NGR 19-005-009, May 1974.

[11]Funai, A. I., "Bidirectional Reflectance Measurements of Specular and Diffuse Surfaces with a Simple Spectrometer," *Progress in Astronautics and Aeronautics: Heat Transfer and Thermal Control*, Vol. 78, edited by A. L. Crosbie, AIAA, New York, 1981, pp. 25–48.

[12]Siegel, R. and Howell, J. R., *Thermal Radiation Heat Transfer*, 2nd ed., Hemisphere, Washington, DC, 1981, pp. 64–72, 127–132, 142–145.

[13]Torrance, K. E. and Sparrow, E. M., "Off-Specular Peaks in the Directional Distribution of Reflected Thermal Radiation," *Journal of Heat Transfer*, Vol. 88C, No. 2, May 1966, pp. 223–230.

[14]Bobco, R. P., "Analytical Determination of Radiation Interchange Factors," Final Rept. NASA NAS9-7980, NASA CR 99683, June 1969.

[15]Bobco, R. P., "Radiation from a Directional Source: Beam Divergence in Solar Simulators," *Journal of Engineering Power*, Vol. 87A, July 1965, pp. 259–269.